Tellus (2000), 52A, 487–499
Printed in UK. All rights reserved

TELLUS
ISSN 0280–6495

Some remarks on the westward propagation of the monsoon depression

By TSING-CHANG CHEN* and JIN-HO YOON, *Atmospheric Science Program, Department of Geological and Atmospheric Sciences, Iowa State University, Ames, Iowa, USA*

(Manuscript received 9 August 1999; in final form 14 February 2000)

ABSTRACT

Several westward propagation properties of the Indian monsoon depression were neglected by previous studies. They include: (1) the slower propagation speed of the depression depicted by a quasi-geostrophic model, (2) the initiation of the asymmetric secondary circulation with respect to the depression center, and (3) the absence of the depression perturbation in the upper troposphere. Some further insights into these neglected propagation properties of the depression are obtained from the streamfunction budget analysis with the ECMWF (European Centre for Medium Range Weather Forecasts) reanalysis data. (1) The inclusion of relative vorticity stretching, which is neglected in a quasi-geostrophic model, increases the depression's westward propagation speed. (2) Within the large-scale environment of the summer monsoon, the coupling of the east–west differentiation of the meridional absolute vorticity advection with the CISK mechanism is conducive to the initiation and development of the asymmetric secondary circulation associated with the depression. (3) The Tibetan high is formed by summertime global-scale stationary waves which are maintained by a Sverdrup balance. The positive streamfunction tendency induced by the upper-tropospheric vortex stretching over the monsoon region suppresses the development of the monsoon depression in the upper troposphere.

1. Introduction

Monsoon depression, a major rain producer in the Indian monsoon system, is a unique synoptic disturbance. This disturbance is characterized by the following special features which pertain to this study.

(1) Monsoon depressions propagate westward against the prevailing monsoon westerlies in the lower troposphere.

(2) Relative vorticity at the center of the monsoon depression can be about two to three times the magnitude of planetary vorticity.

(3) The vertical extent of the monsoon depression may only reach up to 300 mb so that the upper-tropospheric easterlies around the southern rim of the Tibetan high may not exert any significant advection effects on the westward propagation of the monsoon depression.

(4) Most of monsoon depressions are generated over the Bay of Bengal due to the redevelopment of westward-propagating residual lows that moves across Indochina.

Shukla (1978) proposed that CISK (conditional instability of the second kind (Charney, 1973)) barotropic–baroclinic instability is a possible genesis mechanism for monsoon depressions over the Bay of Bengal. Regardless of what may be the actual genesis mechanism, it is well-known that

* Corresponding author.
Corresponding author address: Tsing-Chang (Mike) Chen, Atmospheric Science Program, 3010 Agronomy Hall, Department of Geological and Atmospheric Sciences, Iowa State University, Ames, IA 50011.
e-mail: tmchen@iastate.edu

monsoon depressions are generated primarily by the redevelopment of the westward-propagating residual lows over the Bay of Bengal (Krishnamurti et al., 1977; Saha et al., 1981; Chen and Weng, 1999). Exploring the dynamic processes involved in the development of the monsoon depression, Saha and Chang (1983) showed that a secondary circulation is coupled with this disturbance; ascending motion to the west and descending motion to the east of the center. Later, analyzing the thermal budget of a MONEX (Monsoon Experiment in 1978/79) monsoon depression, Saha and Saha (1988) not only confirmed the aforementioned secondary circulation, but also found that the major rainfall and released latent heat mainly occurred in the west–southwest quadrant of the depression.

As inferred from studies conducted by Saha and his colleagues, there is strong convergence (divergence) to the west (east) of the depression center in the lower troposphere. Thus, vortex stretching induced by the secondary circulation (coupled with the depression) may generate (destroy) vorticity west (east) of the depression center. Presumably, this vorticity production/destruction functions opposite to the horizontal vorticity advection, and also has a larger amplitude than the latter. Based upon the quasi-geostrophic vorticity budget, the net effect of these two dynamic processes results in the westward movement of the depression. This mechanism was introduced by Daggupaty and Sikka (1977) based on the vorticity budget analysis of a monsoon depression and by Sanders (1984) on the quasi-geostrophic streamfunction budget analysis also of a monsoon depression. These diagnostic results are consistent with Krishnamurti et al.'s (1977) theoretical estimation of the westward propagation speed of tropical waves with a length scale similar to the depression, following Matsuno's (1966) linearized tropical wave theory.

In spite of the efforts prior to and post MONEX, some questions concerning the westward propagation of the depression still remain unresolved. They include the following.

(1) Let us denote relative and planetary vorticity as ζ and f, respectively. Since $\zeta/f \sim O(1)$ near the monsoon depression, the quasi-geostrophic model may not be adequate to depict the dynamics of the monsoon depression. As shown by Krishnamurti et al. (1976), the westward propagation speed of the depression simulated by a quasi-geostrophic model is too slow. What mechanism may be missing in this model to reduce the propagation speed?

(2) In previous studies, the quasi-geostrophic streamfunction budget was used to illustrate the possible cause of the depression's westward propagation. If the quasi-geostrophic mechanism is dominant, then why would the secondary circulation coupled with the depression work in the way described by both Saha and Chang (1983) and Saha and Saha (1988)?

(3) The upper-tropospheric easterlies around the southern rim of the Tibetan high have their maximum speeds near $200 \sim 150$ mb. Why is the vertical development of the depression limited to the lower and middle troposphere below 300 mb, preventing the upper-level easterlies from advecting the depression westward?

Answers to the questions posed above would be helpful in understanding the basic dynamics of the monsoon depression. The streamfunction budget derived from a complete vorticity equation, as an extension of Sander's approach, is adopted to examine the first two questions. For the third question, we will explore it from a different perspective. The asymmetric component of the summertime tropical circulation in the upper troposphere is dominated by ultralong waves (Krishnamurti, 1971a, b). Holton and Colton (1972) and Kang and Held (1987) used a simplified streamfunction budget to illustrate the maintenance of these summertime stationary waves. Their approach is incorporated with the streamfunction budget of the depression to search for an answer to the third question.

Although all depressions during the period 1979–94 were analyzed in this study, only the streamfunction budget of the 19–25 June 1979 depression is presented to shed some light on the three questions. The selection of this case based on the following 2 reasons.

(1) There is a clear tendency for most of monsoon depressions to occur during the active monsoon phase (Chen and Weng, 1999). The monsoon life cycle is primarily formed by the modulation of the 30–60 day monsoon mode (Krishsnamurti and Subramanyan, 1982) and the 1979 summer monsoon season has the most pronounced and

organized 30–60 day monsoon mode (even the Indian monsoon was weaker in this summer). These factors constitute a good reason for us to select a monsoon depression during the 1979 active monsoon phase in our presentation.

(2) The data collected during the FGGE (First Global GARP (Global Atmospheric Research Program) Experiment)/MONEX program were the best possible. Thus, many studies (e.g., Sanders, 1984; Warner, 1984; Nitta and Masuda, 1981; Saha and Chang, 1983; Warner and Grumm, 1984; Saha and Saha, 1988; and others) were made to examine various aspects of the 3–8 July 1979 monsoon depression. This depression occurred during the monsoon transition phase (between the active and break monsoon). Instead, the 19–25 June 1979 monsoon depression during the active monsoon phase was selected for illustration.

2. Budget equation and analysis

2.1. *Streamfunction budget equation*

Analyzing the complete vorticity budget of a monsoon depression, Daggupaty and Sikka (1977) pointed out that the vertical advection and tilting terms in the vorticity equation are generally insignificant in comparison with the other terms. After searching through all monsoon depressions, particularly over their west–southwest sectors, for the period 1979–1994, we reached the same conclusion. In addition, recall that $\zeta/f \sim \mathrm{O}(1)$ near the depression. Therefore, we may simplify the vorticity equation into the following form:

$$\frac{\partial \xi}{\partial t} + u\frac{\partial \zeta}{\partial x} \underbrace{+ v\frac{\partial \zeta}{\partial y}}_{①} + v\beta = -f\nabla\cdot V \underbrace{- \zeta\nabla\cdot V}_{②} + F \tag{1}$$

In the midlatitudes, $\zeta/f \sim \mathrm{O(Ro)}$ where Ro is Rossby number. Both terms ① and ② are generally neglected in a linearized quasi-geostrophic model. Since $\zeta/f \sim \mathrm{O}(1)$ near the depression, we keep these two terms, which are comparable in magnitude to their counterparts of planetary vorticity, in the monsoon region. The inverse Laplace transform of eq. (1) gives us the streamfunction budget equation:

$$\psi_t = \underbrace{\nabla^{-2}\left(-u\frac{\partial \zeta}{\partial x}\right)}_{\psi_{Ax}} + \underbrace{\nabla^{-2}\left(-v\frac{\partial \zeta}{\partial y}\right)}_{\psi_{Ay}} + \underbrace{\nabla^{-2}(-v\beta)}_{\psi_{A\beta}} + \underbrace{\nabla^{-2}(-f\nabla\cdot V)}_{\psi_{\chi f}} + \underbrace{\nabla^{-2}(-\zeta\nabla\cdot V)}_{\psi_{\chi\zeta}} + \underbrace{\nabla^{-2}F}_{\psi_F}. \tag{2}$$

or

$$\psi_t = \psi_A + \psi_\chi + \psi_F, \tag{3}$$

where $\psi_A \equiv \psi_{Ax} + \psi_{Ay} + \psi_{A\beta}$ and $\psi_\chi \equiv \chi_{\chi f} + \psi_{x\zeta}$. Compared to Sander's quasi-geostrophic streamfunction budget equation, $\psi_{\chi\zeta}$ is an extra quantity. In his budget analysis of a MONEX depression, Sanders (1984) showed that ψ_A almost vanishes. It will be shown later that ψ_{Ay} and $\psi_{A\beta}$ exhibit a spatial structure similar to each other, but generally opposite to ψ_{Ax}. Although magnitudes of ψ_{Ay} and $\psi_{A\beta}$ are individually somewhat smaller than ψ_{Ax}, the latter quantity is almost counterbalanced by the two former quantities. ψ_χ is mainly determined by horizontal divergence which is linked to vertical motion through the continuity equation. It was shown by Krishnamurti (1968) and Daggupaty and Sikka (1977) that vertical motion can be affected by surface friction and diabatic heating. Although these two quantities do not show up explicitly in eqs. (1) and (2), they can affect ψ_χ through horizontal divergence. At any rate, in order to understand how various dynamic processes affect the westward movement of a monsoon depression, we will analyze the budget expressed by eq. (2).

2.2. *Analysis*

In order to save space, the complete streamfunction budget (eq. (2)) for a typical monsoon depression on a given day is presented, instead of its entire life cycle (even though many cases were analyzed), for illustration. The depression extends up to only 300 mb exhibiting its maximum amplitude at about 850 mb. Thus we will focus on this level.

Monsoon depressions are mobile synoptic disturbances embedded in the quasi-stationary global-scale summer circulation in the tropics. To illustrate the depression's westward propagation, Krishnamurti et al. (1977) divided the *x–t* diagram of surface pressure into the long (1–2) and short

(3–12) wave regimes. The depression's horizontal scale ($\sim$3000 km) is roughly equivalent to waves 12–13 at 20°N. To facilitate our illustration of dynamic processes involved in the depression's development and westward movement, a scale separation is therefore adopted to divide the streamfunction budget into two regimes: long (1–5)- and short (6–25)-wave regimes. Any variable ( ) of the former wave regime is denoted by $(\ )^{\mathrm{L}}$, while that of the latter wave regime by $(\ )^{\mathrm{S}}$. The x–t diagrams of both ψ^{L} (850 mb) and ψ^{S} (850 mb) are shown in Fig. 1. The 30–60 day oscillation of the Indian monsoon circulation is reflected by the long-wave regime. As indicated by the marked trajectories in Fig. 1b, the depressions move westward following negative ψ^{S} (850 mb) anomalies. Thus, the 850-mb streamfunction budget of a MONEX depression on 24 June 1979 in the short-wave regime shown in Fig. 2 will be used to answer the first two questions.

3. Results and discussion

3.1. *Question 1. Slower depression's propagation in a quasi-geostrophic model*

(1) As guided by our intuition, the depression should be advected eastward by the monsoon westerlies. This intuitive perspective may be supported by the spatial structure of ψ^{S}_{Ax} (Fig. 2b) with *negative* (positive) values east (west) of the depression center (indicated by a cross in Fig. 2a). Evidently the streamfunction tendency induced by the zonal vorticity advection $(-u\,\partial\zeta/\partial x)$ enables the depression to move *eastward*.

(2) Other terms in eq. (2), ψ^{S}_{Ay}, $\psi^{\mathrm{S}}_{A\beta}$, $\psi^{\mathrm{S}}_{\chi f}$, and $\psi^{\mathrm{S}}_{\chi\zeta}$ (Figs. 2c–f) are all almost spatially in phase with *negative* (positive) values to the west of the depression center, i.e., opposite to the spatial structure of ψ^{S}_{Ax}. In other words, all dynamic processes, except ψ_{Ax}, expressed in eq. (2) tend to move the depression westward.

Recall that the barotropic streamfunction budget equation may be written as

$$\psi^{\mathrm{S}}_t \simeq \psi^{\mathrm{S}}_{Ax} + \psi^{\mathrm{S}}_{Ay} + \psi^{\mathrm{S}}_{A\beta} (= \psi^{\mathrm{S}}_A). \tag{4}$$

As found by Daggupaty and Sikka (1977) in their vorticity budget analysis, and Sanders (1984) in his quasi-geostrophic streamfunction budget analysis, the quantity ψ_A is approximately zero. This means that the zonal vorticity advection is nearly counterbalanced by the meridional advection of total vorticity. For this reason, it is not surprising to see that *the depression simulated by Krishnamurti et al. (1976) with a barotropic model is essentially stationary*. This argument is supported by the small magnitude of ψ^{S}_A (compared to ψ^{S}_x) over the Indian subcontinent and the head Bay of Bengal (Fig. 2h). The quasi-geostrophic streamfunction budget equation (if not linearized) is

$$\psi^{\mathrm{S}}_t \simeq \psi^{\mathrm{S}}_{Ax} + \psi^{\mathrm{S}}_{Ay} + \psi^{\mathrm{S}}_{A\beta} + \psi^{\mathrm{S}}_{xf} (= \psi^{s}_A + \psi^{\mathrm{S}}_{xf}), \tag{5}$$

where $\psi^{\mathrm{S}}_{x\zeta}$ is not included. Compared to the depression represented by negative values of ψ^{S} over the Bay of Bengal (Fig. 2a), the westward movement of the depression is inferred by the negative values of streamfunction tendency $(\psi^{\mathrm{S}}_A + \psi^{\mathrm{S}}_{\chi f})$ (Fig. 2k). It is shown in Fig. 2f that the amplitude of $\psi^{\mathrm{S}}_{\chi\zeta}$ is comparable to all westward driving processes, ψ^{S}_{Ay}, $\psi^{\mathrm{S}}_{A\beta}$, and $\psi^{\mathrm{S}}_{\chi f}$. *The missing term $\chi^{\mathrm{S}}_{\chi\zeta}$ in the quasi-geostrophic model certainly reduces the westward propagation speed of depressions depicted by this model*, as revealed by the contrast between $(\psi^{\mathrm{S}}_A + \psi^{\mathrm{S}}_{\chi f})$ (Fig. 2k) and $(\psi^{\mathrm{S}}_A + \psi^{\mathrm{S}}_{\chi})$ (Fig. 2l).

3.2. *Question 2. Westward movement of depression*

Based upon our answer to Question 1, the streamfunction budget equation may be approximated by

$$\psi^{\mathrm{S}}_t \simeq \psi^{\mathrm{S}}_{\chi f}. \tag{6}$$

The spatial structure of $\psi^{\mathrm{S}}_{\chi f}[=\nabla^{-2}(-f\nabla\cdot V)^{\mathrm{S}}]$, streamfunction tendency induced by vortex stretching (Fig. 2e), is determined by that of the secondary circulation coupled with a depression: convergence west of and divergence east of the depression center in the lower troposphere. According to eq. (6), the westward movement of the depression is the result of the structure of the secondary circulation. However, previous studies have not seriously questioned the following basic issue: Why is the secondary circulation formed in such a manner? The answer to this question may possibly disclose the mechanism responsible for moving the monsoon depression westward.

Analyzing the baroclinic process and the thermal budget maintaining the monsoon depression, Saha and his colleagues showed that warm (cold) air advection exists west (east) of the depression

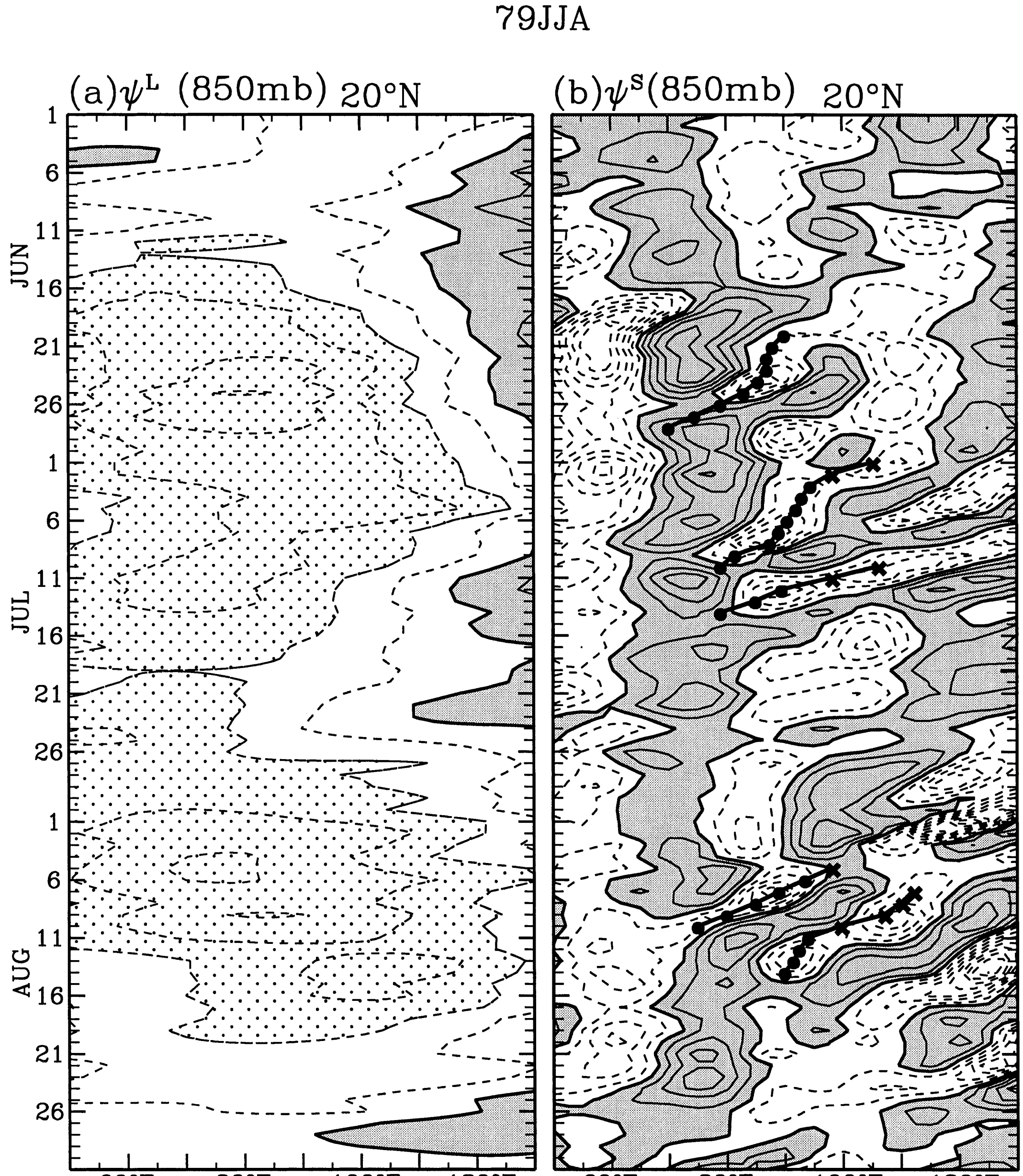

Fig. 1. The *x–t* diagrams of (a) ψ^L (850 mb) and (b) ψ^S (850 mb) at 20°N over the monsoon region. Superscripts L and S represent the long (1–5) and short (6–25) wave regimes. The daily longitudinal location of residual lows (×) and monsoon depression (●) are superimposed on the *x–t* diagram of ψ^S (850 mb). Positive values of both ψ^L (850 mb) and ψ^S (850 mb) are stippled. Contour intervals of these two variables are $4 \times 10^6\ m^2\ s^{-1}$ and $10^6\ m^2\ s^{-1}$, respectively. In order to make the intraseasonal oscillation of ψ^L (850 mb) discernible, the ψ^L (850 mb) values smaller than $8 \times 10^6\ m^2\ s^{-1}$ are lightly stippled.

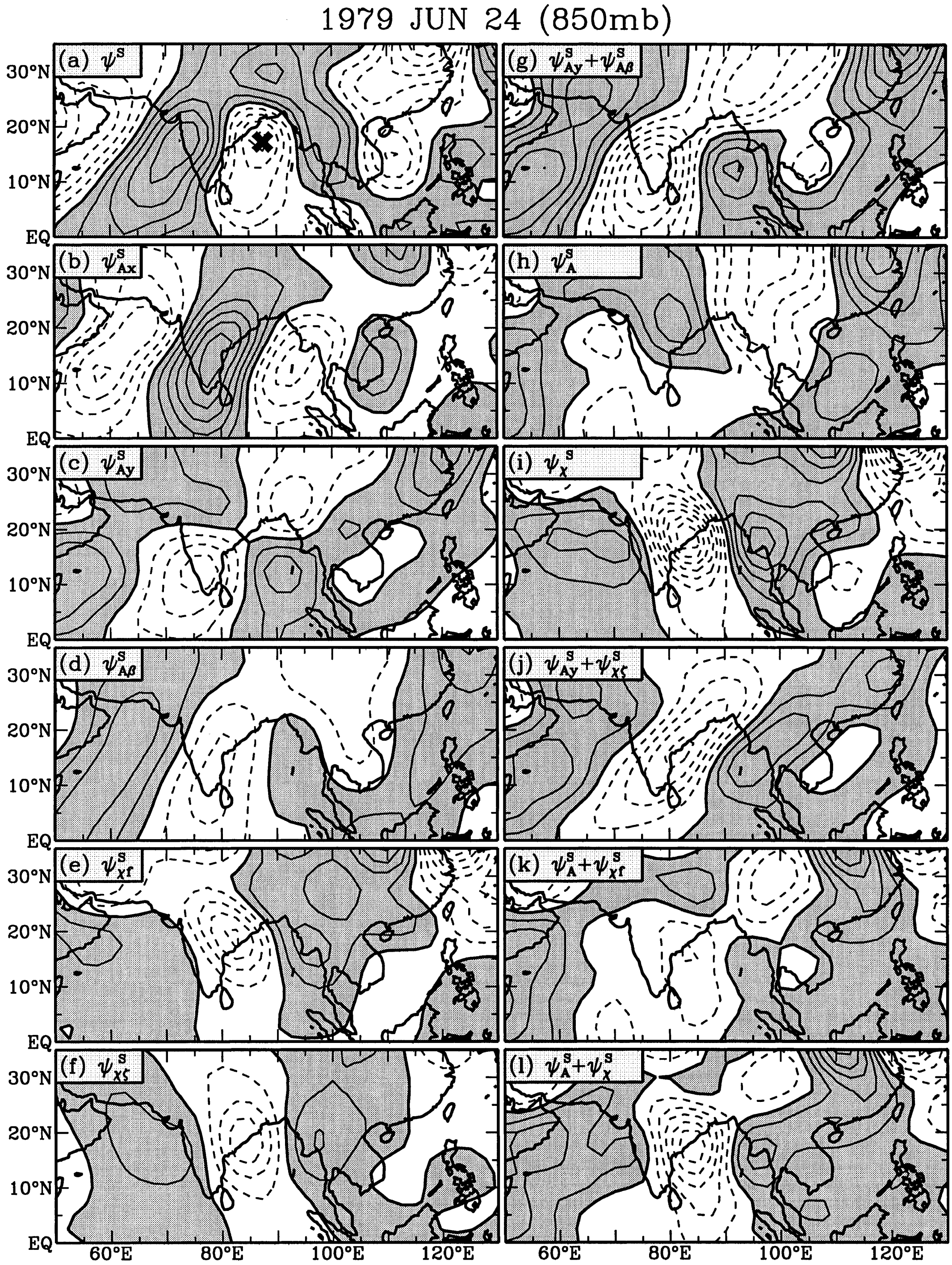

Fig. 2. Streamfunction budget analysis of the short-wave regime at 850 mb: individual terms and the combination of some terms in eq. (2). Positive values are stippled, and the contour intervals of ψ^S (850 mb) and other quantities are 2×10^6 m^2 s^{-1} and 20 m^2 s^{-2} respectively.

center, while rainfall occurs primarily over the south–southwest sector. The secondary circulation is evidently maintained by these thermal processes. In other words, Saha and his colleagues' studies give us a clear view of the maintenance of the secondary circulation, instead of the mechanism to induce it. Therefore, an initiation mechanism of this secondary circulation is proposed.

The proposed initiation mechanism of the asymmetric secondary circulation associated with the depression is derived from the chronological development of the depression (Fig. 3). The depression development is highlighted by the following three phases:

(1) Initial phase

The depression was formed on 19 June 1979 (the top panel of Fig. 3a) when a residual low reached the west coast of Bangladesh. The intensification of cyclonic flow associated with the residual low results in the enhancement of *southward* (northward) meridional vorticity advection (i.e., $-v\,\partial\zeta/\partial y$ and $-v\beta$) to the west (east) of the newly formed depression. Therefore, both ψ^S_{Ay} and $\psi^S_{A\beta}$ induce negative (positive) streamfunction tendency in the western (eastern) section of the depression (like the case shown in Fig. 2a). Recall that ψ^S_{Ax} (Fig. 2b) and $(\psi^S_{Ay}+\psi^S_{A\beta})$ (Fig. 2g) exhibit an opposite polarity in spatial structure. The negative values of ψ^S_A over the Bay of Bengal (the top panel of Fig. 3b) indicate that the former streamfunction tendency is dominated by the latter one. Since ψ^S_x (the top panel of Fig. 3c) is weak and unorganized over the Bay of Bengal at the initial stage, the development and westward movement of the depression at this stage is primarily driven by east–west differentiation of $(\psi^S_{Ay}+\psi^S_{A\beta})$. A secondary circulation associated with the depression may possibly be induced by this east–west differentiation of $(\psi^S_{Ay}+\psi^S_{A\beta})$ coupled with CISK. To substantiate this argument, we superimpose the 850-mb streamline charts (Fig. 3a) with the precipitation estimation generated by Susskind et al. (1997) of Goddard Space Flight Center. The newly initiated monsoon depression is attached to a trough line along the west coast of Burma (currently Maynmar). The rainfall estimation shows that a small center is located west of this trough line (although slightly south of the depression center). As inferred from this rainfall distribution, the induced secondary circulation associated with this depression would have its upward (downward) branch west (east) of the trough line.

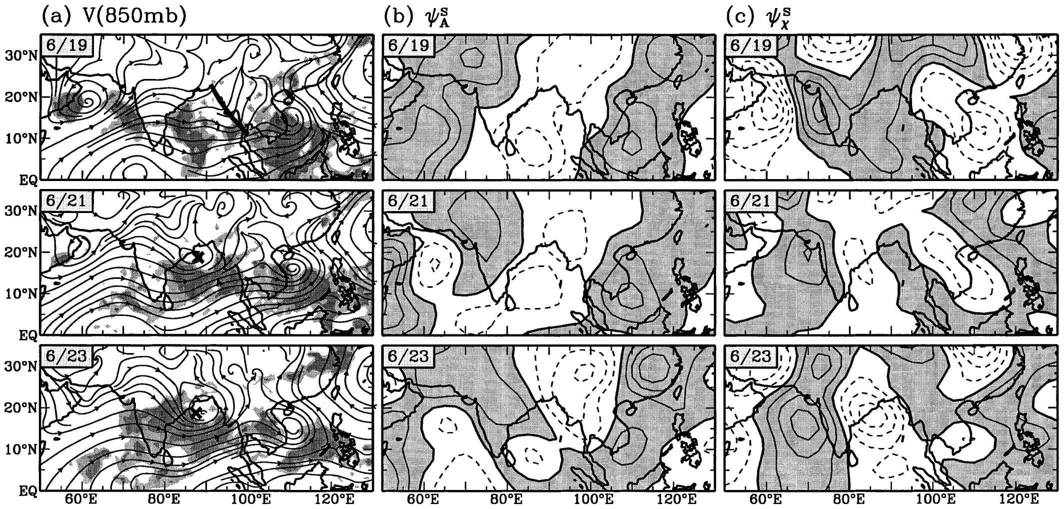

Fig. 3. Chronological development of the 24 June 1979 monsoon depression before its maximum intensity: (a) daily 850-mb streamline charts superimposed with Susskind et al.'s (1997) precipitation estimation, (b) daily ψ^S_A (850 mb), and (c) daily ψ^S_χ (850 mb). The depression center is marked by a cross on the streamline charts. Precipitation larger than 20 (15) mm day^{-1} is heavily (lightly) stippled. The stippling convention and contour intervals of ψ^S_A and ψ^S_χ n Fig. 2 is adopted.

(2) Transition phase

Two days (21 June 1979) after its genesis, the depression has moved westward and formed a vortex near the northeast coast of the Indian subcontinent with significant rainfall in the southwest quadrant of the depression (the middle panel of Fig. 3a). ψ^S_χ became organized with negative (positive) values west (east) of the depression center (the middle panel of Fig. 3c). As inferred from the spatial structure of ψ^S_χ, the CISK initiated by the east–west differentiation of $(\psi^S_{Ay}+\psi^S_{A\beta})$ initiates the asymmetric circulation with respect to the depression. Ascending (descending) motion west (east) of the depression center. During this phase, ψ^S_A became a secondary influence on the monsoon depression.

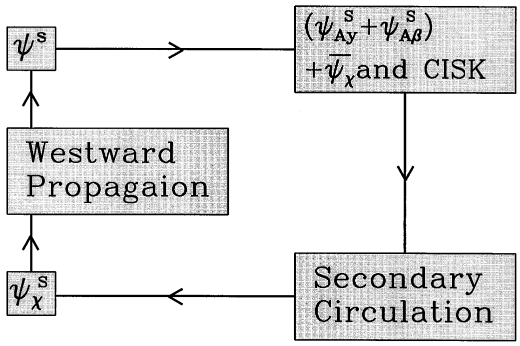

Fig. 4. A schematic diagram summarizing the possible effect of the east–west differentiation of $(\psi_{Ay}+\psi_{A\beta})$ on the initiation of the secondary circulation associated with the monsoon depression.

(3) Mature phase

In the following 2 days, the depression moved slightly westward and reached maturity. Over the head Bay of Bengal, ψ^S_A became much less organized and functioned dynamically opposite to its own role in the initial phase of the depression (the top panel of Fig. 3b). In other words, ψ^S_{Ax} is slightly overbalanced by $(\psi^S_{Ay}+\psi^S_{A\beta})$. Thus, ψ^S_A may move the depression eastward. However, compared to ψ^S_A in structure and magnitude, ψ^S_χ becomes the major dynamic process to move the depression westward. It is inferred from the well developed and organized structure of ψ^S_χ that the asymmetric circulation associated with the depression is well developed and coincided with the rainfall distribution during this phase.

So far, the contribution of the long-wave regime to the depression's streamfunction budget (will be shown in the next section) has not been considered. Actually, ψ^L_χ is negative in the lower troposphere over the monsoon region. The vortex stretching associated with the long-wave regime maintains the monsoon trough in this region. Evidently, the long-wave environment is conducive to the depression's development, and in turn, the secondary circulation. Based upon the chronological development of the depression shown in Fig. 3, our answer to Question 2, i.e., the initiation mechanism of the secondary circulation associated with the depression, may be summarized by the simple schematic diagram in Fig. 4. *The asymmetric secondary circulation with respect to the depression center is initiated by the coupling of CISK with the east–west differentiation of* $(\psi^S_{Ay}+\psi^S_{A\beta})$ *and the existence of* $\bar{\psi}_\chi$, where $(\overline{})$ is the long-term summer mean value of ( ).

3.3. *Question 3. Limited vertical development of monsoon depression*

To explore the cause of its westward propagation, Krishnamurti et al. (1977) treated monsoon depressions as tropical wave disturbances with a small horizontal scale in the lower troposphere. Analyzing the 850-mb quasi-geostrophic streamfunction budget, Sanders (1984) showed that the westward movement of the monsoon depression may be caused by vortex stretching induced by the secondary circulation associated with this depression. These studies offer some explanation to this puzzling westward propagation against the lower-tropospheric monsoon westerlies (Sikka, 1977), but what is the propagation property of this disturbance in the middle and upper troposphere? Daggupaty and Sikka (1977) examined the depression in the real atmosphere, while Shukla (1978) used only the long-term zonal mean flow (with a vertical phase reversal at about 400–500 mb) in his model. Recall that the global scale summertime circulation in the tropics is dominated by waves 1–2 (Krishnamurti, 1979) which exhibit a vertical phase reversal at about 400–500 mb (White, 1982). Evidently, the summertime stationary waves are missing in Shukla's basic flow. Can this missing element be the basic cause of the vertical limit of the monsoon depression? The maintenance of summertime stationary waves in the tropics is examined to search for an answer to this question.

The atmospheric circulation in the northern-hemisphere tropics and subtropics during the summer season is characterized in the upper troposphere by the Tibetan high and the North Pacific and North Atlantic oceanic troughs (Fig. 5a), and in the lower troposphere by the Indian monsoon trough and the North Pacific and North Atlantic anticyclone (Fig. 5c). It is inferred from the contrast between Figs. 5a and c that a vertical phase reversal of the tropical stationary wave should occur in the middle troposphere. This inference is confirmed by the zonal height cross-section of the eddy streamfunction at 20°N, $\bar{\psi}_E$ (20°N) (Fig. 5b), as a monsoon characteristic of the tropical circulation observed by White (1982). Note that $(\ )_E = (\ ) - (\ )_Z$, where $(\ )_Z$ is zonal average of $(\ )$ around a latitudinal circle. The vertical phase reversal in tropical stationary waves across the

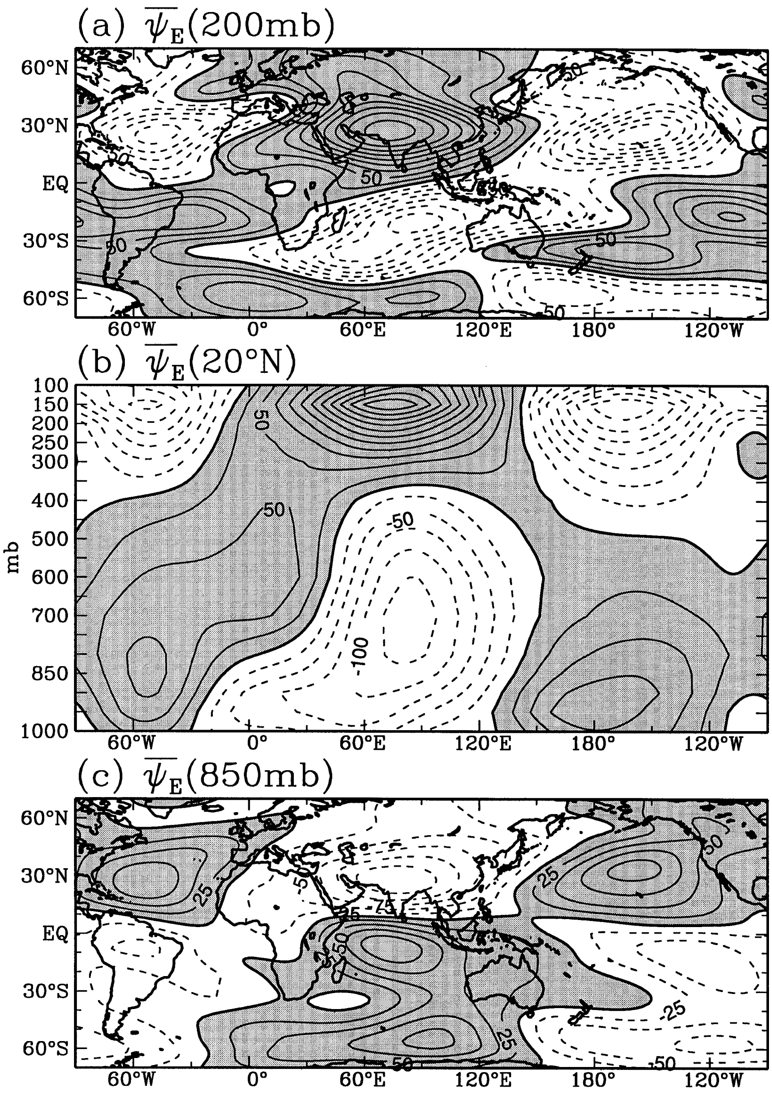

Fig. 5. Structure of summertime stationary waves depicted by streamfunction: (a) $\bar{\psi}_E$ (200 mb), (b) zonal-height cross-section of $\bar{\psi}_E$ (20°N) and (c) $\bar{\psi}_E$ (850 mb). Positive values of $\bar{\psi}_E$ are stippled. Contour interval of $\bar{\psi}_E$ is 2×10^6 m^2 s^{-1}.

monsoon region may constitute a large-scale environment restrictive to the vertical development of the monsoon depression. In other words, the Indian monsoon trough (Tibetan high) may synoptically facilitate (hinder) the growth of the monsoon depression in the lower (upper) troposphere. This argument may be substantiated by performing the streamfunction budget analysis on stationary waves in the tropics.

Holton and Colton (1972) suggested that summer stationary waves in the tropics are maintained by the balance between the horizontal advection of vorticity and vortex stretching. In order to satisfy this balance, vorticity and divergence centers (i.e., centers of streamfunction and velocity potential) should be spatially in quadrature. Analyzing Krishnamurti's (1971b) tropical summer wind at 200 mb, Holton and Cotton could not obtain this balance. Therefore, they suggested that the imbalance in the vorticity budget of stationary wave should be dissipated by the vertical transport of vorticity by cumulus convection. In contrast, Kang and Held (1986) found that global-scale summer stationary waves in the tropics simulated by a global model are maintained by a Sverdrup balance instead. As inferred from $\bar{\psi}_E$ in Fig. 5a and $\bar{\psi}_{\chi f}$ in Fig. 6b, a spatial quadrature relationship does exist between $\bar{\psi}_E$ and $\bar{\chi}_E$ in the real atmospheric circulation. The opposite polarity between $\bar{\psi}_{A\beta}$ (200 mb) (Fig. 6a) and $\bar{\psi}_{\chi f}$ (Fig. 6b) clearly shows the existence of a Sverdrup balance. For further discussion, a zonal-vertical cross-section of $\bar{\psi}_{\chi f}$ (20°N) is displayed in Fig. 6c. Over the monsoon region, the vortex stretching induced by the divergent circulation results in negative (positive) streamfunction tendency in the lower (upper) troposphere. The vertical phase reversal of $\bar{\psi}_{\chi f}$ (20°N) is coincident with $\bar{\chi}$ (20°N) (not shown). Evidently, negative $\bar{\psi}_{\chi f}$ in the lower troposphere facilitate the development/deepening of the monsoon depression in this region. On the contrary, positive $\bar{\psi}_{\chi f}$ in the upper troposphere hinders/dissipates the development of the monsoon depression. To substantiate this argument in a more quantitative way, i.e., to measure the effect of the summertime stationary waves on the development of the monsoon depression, vertical cross-sections of v (85°E) and ψ_χ^S (20°N) are displayed in Figs. 7a and b, respectively.

The center of the depression is denoted by a thick tick mark. As revealed by the v (20°N) cross-section, the depression does not reach the upper troposphere. Comparing maximum values of ψ_χ^S (20°N) in the lower troposphere and $\bar{\psi}_{\chi f}$ (20°N) in the upper troposphere, we conclude $\psi_\chi^S + \bar{\psi}_{\chi f} > 0$ in the upper troposphere. It is inferred from this comparison that positive $\bar{\psi}_{\chi f}$ in the upper troposphere is more than sufficient to counterbalance negative ψ_χ^S, namely to suppress the possible generation of the negative ψ^S tendency associated with the monsoon depression. For our information, we actually computed $\psi_{\chi f}^L$ (20°N) on 24 June (not shown). It turned out that the daily vertical structure and magnitude of this quantity did not differ significantly from $\bar{\psi}_{\chi f}$. In summary, *the limited vertical development of the monsoon depression is attributed to the suppression by the upper-tropospheric high system over the monsoon region.*

4. Concluding remarks

Synoptic cyclones in the midlatitudes are advected by the prevailing westerlies, while synoptic disturbances (including easterly, equatorial, and African waves) in the tropics are transported by the tropical easterlies. In contrast, monsoon depressions over the Indian monsoon region propagate westward against the lower-tropospheric monsoon westerlies. Regardless of the possible contribution of the upper easterlies to their westward propagation, the limited vertical extent of the monsoon depression (only up to 300 mb) prevents this advection effect. Although a number of studies has been performed to explore the possible causes of the depression's westward movement, we still identified three unresolved questions concerning the depression's propagation properties: (1) Why is the actual westward propagation speed faster than that depicted by a quasi-geostrophic model? (2) What is the possible mechanism to form the secondary circulation of a monsoon depression in such a way to make it move westward? (3) Why is the depression's vertical development limited? The findings of this study are as follows.

(1) Since $\zeta/f \sim O(1)$ in a monsoon depression, meridional advection $(-v\,\partial\zeta/\partial y)$ and stretching $(-\zeta\nabla\cdot V)$ of relative vorticity in the vorticity budget equation become comparable in magnitude to meridional advection $(-v\beta)$ and stretching

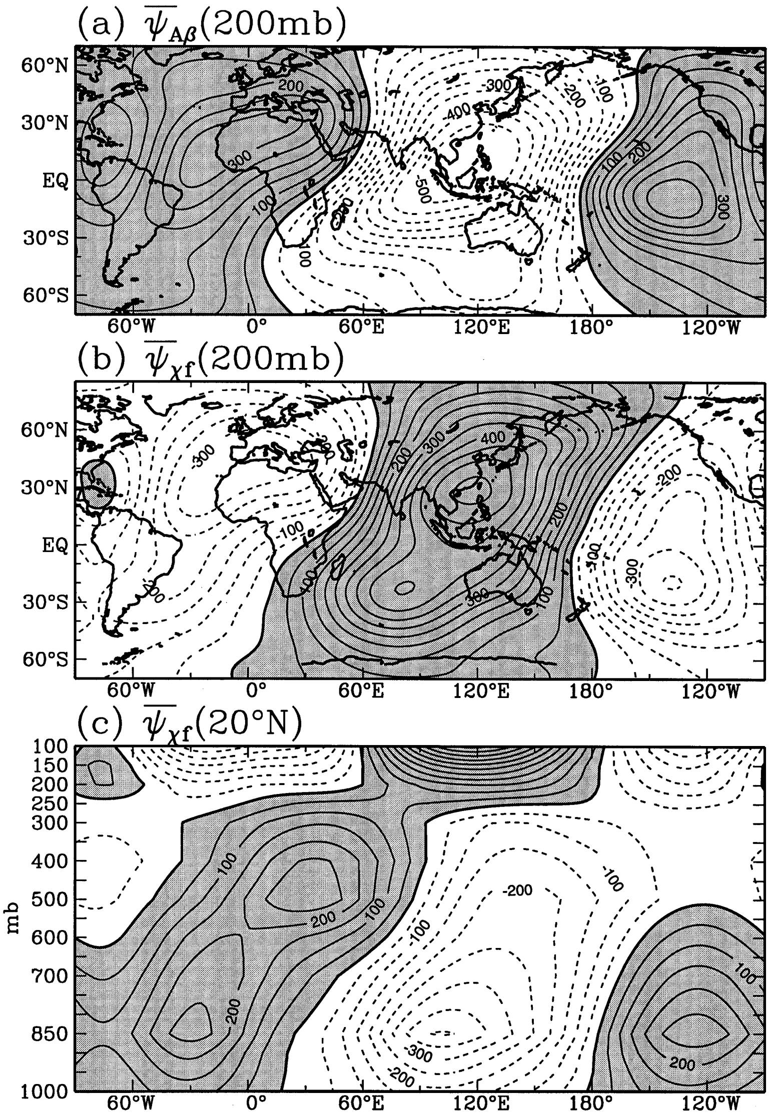

Fig. 6. Streamfunction budget of summertime stationary waves: horizontal charts of (a) $\bar{\psi}_{A\beta}$ (200 mb) and (b) $\bar{\psi}_{\chi f}$ (200 mb), and (c) zonal-height cross-section of (20°N). Positive values of both $\bar{\psi}_{A\beta}$ and $\bar{\psi}_{\chi f}$ are stippled. Contour intervals for all variables are 50 m^2 s^{-2}.

$(-f\nabla \cdot V)$ of planetary vorticity. Therefore, streamfunction tendencies induced by the former two dynamic processes, ψ_{Ay} and $\psi_{\chi\zeta}$, enable the depression to move westward. Elimination of these 2 processes in a linearized quasi-geostationary model results in slower propagation speeds in the model.

(2) The following was observed in our analysis of the monsoon depression:

$\psi_A^S (= \psi_{Ax}^S + \psi_{Ay}^S + \psi_{A\beta}^S) \simeq 0.$

Thus, the vortex stretching becomes the major dynamic process in moving a depression westward. Because the vortex stretching is induced by the secondary circulation associated with a monsoon depression, the depression's westward propagation is primarily determined by the spatial structure of the secondary circulation: upward (downward) motion to the west (east) of the depression center. Over the monsoon region, the monsoon trough in the lower troposphere is maintained by the vortex stretching of summertime stationary waves. Following the chronological development of the monsoon depression before its maximum intensity, the east–west differentiation of $(\psi_{Ay}+\psi_{A\beta})$ coupled with the CISK mechanism within the monsoon trough is conducive to the initial development of the secondary circulation.

(3) The vertical development of a monsoon depression in the upper troposphere is suppressed by the Tibetan high. This vertically limited development of a depression can be illustrated through streamfunction budget analysis: $\psi_\chi^S+\bar{\psi}_{\chi f}>0$.

Monsoon depressions bring to the Indian subcontinent more than half of its monsoon rainfall. The accurate forecasting of the monsoon depression's movement is important over this subcontinent not only to agriculture production, but also to a number of other human activities. Findings in this study indicate that numerical simulations of the monsoon depression and its movement can be significantly improved by carefully considering the following factors: (1) non-linear processes including meridional advection and stretching of relative vorticity; (2) a proper simulation of the secondary circulation associated with the depression; (3) summertime stationary waves forming the Tibetan anticyclone in the upper troposphere.

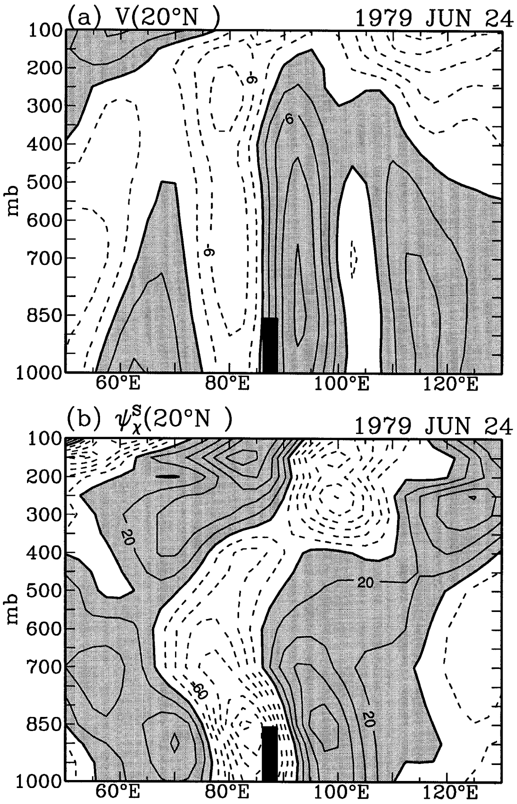

Fig. 7. (a) Vertical structure of 24 June 1979 MONEX depression depicted by the meridional wind cross-section at 20°N, versus (85°E), and (b) vertical cross-section of the streamfunction tendency induced by the vorticity flux divergence in the short-wave regime at 20°N, ψ_χ^S (20°N). Positive values of v and ψ_χ^S are stippled. Contour intervals of these two variables are 3 m s^{-1} and 20 m^2 s^{-2}, respectively. The center of the depression is denoted by a thick tick mark.

5. Acknowledgements

This study is supported by the NSF Grant ATM-9906454. Comments and suggestions offered by two reviewers are very helpful in improving this paper. Typing support provided by Mrs. Reatha Diedrichs and editing assistance by Mr. Seth Loyd are highly appreciated.

REFERENCES

Charney, J. G. 1973. Movable CISK. *J. Atmos. Sci.* **30**, 50–52.

Chen, T.-C. and Chen, J.-M. 1990. On the maintenance of stationary eddies in terms of the streamfunction budget analysis. *J. Atmos. Sci.* **47**, 2818–2824.

Chen, T.-C. and Weng, S.-P. 1999. Interannual and intraseasonal variations in monsoon depressions and their westward-propagating predecessors. *Mon. Wea. Rev.* **127**, 1005–1020.

Chen, T.-C. and Weng, S.-P. 1999. Maintenance of austral summertime upper-tropospheric circulation over tropical South America: The Bolivian high-Nordeste low system. *J. Atmos. Sci.* **56**, 2081–2100.

Daggupaty, S. M. and Sikka, D. R. 1977. On the vorticity budget and vertical velocity distribution associated with the life cycle of a monsoon depression. *J. Atmos. Sci.* **34**, 773–792.

Holton, J. R. and Colton, D. E. 1972. A diagnostic study of the vorticity balance at 200 mb in the tropics during the northern summer. *J. Atmos. Sci.* **29**, 1124–1128.

Kang, I.-S. and Held, I.-M. 1986. Linear and nonlinear diagnostic models of stationary eddies in the upper troposphere during northern summer. *J. Atmos. Sci.* **43**, 3045–3057.

Krishnamurti, T. N. 1968. A diagnostic balance model for studies of weather systems of low and high latitudes, Rossby number less than 1. *Mon. Wea. Rev.* **96**, 197–207.

Krishnamurti, T.-N. 1971a. Tropical east–west circulations during the northern summer. *J. Atmos. Sci.* **28**, 1342–1347.

Krishnamurti, T.-N. 1971b. Observational study of the tropical upper tropospheric motion field during the Northern Hemisphere summer. *J. Appl. Meteor.* **10**, 1066–1096.

Krishnamurti, T.-N. 1979. *Tropical meteorology*. Compendium of meteorology (II). WMO Rep. 364, 428 pp. (Available from World Meteorological Organization. Case Postale 2300. CH-1211, Geneva, Switzerland.)

Krishnamurti, T.-N. and Subrahnanyam, D. 1982. The 30–60 day mode at 850 mb during MONEX. *J. Atmos. Sci.* **39**, 2088–2095.

Krishnamurti, T.-N., Molinari, J., Pan, H. and Wong, V. 1977a. Downstream amplification and formation of monsoon disturbances. *Mon. Wea. Rev.* **105**, 1281–1297.

Krishnamurti, T.-N., Kanamitsu, M., Godbale, R., Chang, C. B., Carr, F. and Chow, J. H. 1976. Study of a monsoon depression (II), dynamical structure. *J. Meteor. Soc. Japan* **54**, 208–226.

Matsuno, T. 1976. Quasi-geostrophic motions in the equatorial area. *J. Meteor. Soc. Japan* **53**, 227–240.

Nitta, T. and Masuda, K. 1981. Observational study of a monsoon depression developed over the Bay of Bengal during summer MONEX. *J. Meteor. Soc. Japan* **59**, 672–682.

Saha, K. and Chang, C.-P. 1981. The baroclinic processes of monsoon depressions. *Mon. Wea. Rev.* **111**, 1506–1514.

Saha, K. and Saha, S. 1988. Thermal budget of a monsoon depression in the Bay of Bengal during FGGE-MONEX 1979. *Mon. Wea. Rev.* **116**, 242–254.

Saha, K., Sanders, F. and Shukla, J. 1981. Westward propagating predecessors of monsoon depressions. *Mon. Wea. Rev.* **109**, 330–343.

Sanders, F. 1984. Quasi-geostrophic diagnosis of the monsoon depression of 5–8 July 1979. *J. Atmos. Sci.* **41**, 538–552.

Shukla, J. 1978. CISK-barotropic-baroclinic instability and the growth of monsoon depressions. *J. Atmos. Sci.* **35**, 495–508.

Sikka, D. R. 1977. Some aspects of the life history, structure and movement of monsoon depressions. *Pure and Applied Geophysics* **115**, 1501–1529.

Susskind, J., Piraino, P., Rokke, L., Iredell, L. and Mehta, A. 1997. Characteristics of the TOVS pathfinder path A dataset. *Bull. Amer. Meteor. Soc.* **78**, 1449–1472.

Warner, C. 1984. Core structure of a Bay of Bengal monsoon depression. *Mon. Wea. Rev.* **112**, 137–152.

Warner, C. and Grumm, R. H. 1984. Cloud distributions in a Bay of Bengal monsoon depression. *Mon. Wea. Rev.* **112**, 153–172.

White, G. H. 1982. An observational study of the Northern Hemisphere extratropical summertime general circulation. *J. Atmos. Sci.* **39**, 28–40.